Conformational Behavior of Aza-*C*-Glycosides: Experimental Demonstration of the Relative Role of the *exo-anomeric* Effect and 1,3-Type Interactions in Controlling the Conformation of Regular Glycosides

Juan Luis Asensio,[†] F. Javier Cañada,[†] Alicia García-Herrero,[†] María T. Murillo,[†] Alfonso Fernández-Mayoralas,[†] Brian A. Johns,[‡] Janusz Kozak,[‡] Zhenzyu Zhu,[‡] Carl R. Johnson,*[,‡] and Jesús Jiménez-Barbero*[,†]

Contribution from the Instituto de Química Orgánica, CSIC, Juan de la Cierva 3, 28006 Madrid, Spain, and Department of Chemistry, Wayne State University, Detroit, Michigan 48202-3489

Received July 1, 1999. Revised Manuscript Received September 24, 1999

Abstract: The conformational behavior of different aza-*C*-glycosides synthesized as glycosidase inhibitors has been studied using a combination of NMR spectroscopy (*J* and NOE data) and time-averaged restrained molecular dynamics calculations. The obtained results show that the population distribution of conformers around their pseudoglycosidic linkages is mainly controlled by 1,3-*syn*-diaxial interactions. Electrostatic effects slightly modulate the conformational equilibrium. This result is in contrast with that observed for *O*-glycosides. For these natural compounds, the conformational behavior around the glycosidic linkage Φ is mainly governed by the *exo-anomeric* effect. Experimentally based energy values for both the 1,3-*syn*-diaxial interactions and the stereoelectronic effect have been deduced. Finally, the inhibitory activity of these compounds has been tested again a variety of glycosidase enzymes.

Introduction

Carbohydrate−protein interactions are involved in a wide range of biological activities starting from fertilization and extending to pathological processes such as tumor spread.[1,2] Since the carbohydrate ligands are object of hydrolytic attacks, *C*-glycosides have been developed which afford the possibility for improved chemical and biochemical stability.[3,4] However, the methylene-bridged analogues do not simply behave as noncleavable glycosides, as differences between the behavior of *C*- and *O*-glycosides have been reported.[5] In addition, since the substitution of an oxygen by a methylene group results in a change in both the size and the electronic properties of the glycosidic linkage,[6] the flexibility around the Φ/Ψ torsion angles can be markedly changed.[7] Thus, the *exo-anomeric* effect,[8] due to the presence of the interglycosidic oxygen atom, disappears in the *C*-glycoside[9] along with a consequent variation of the steric interactions between both residues. Kishi and co-workers have been very active in this field and on the basis of a qualitative analysis of NMR data[10] have proposed that *C*- and *O*-glycosides share the same conformational characteristics in solution.[10,11] Moreover, the recent finding that the conformation of *C*-lactose bound to peanut agglutinin is basically identical to the conformation of its parent *O*-lactose bound to the same

[†] Instituto de Química Orgánica.

[‡] Wayne State University.

(1) *Glycosciences: Status and Perspectives*; Gabius, H. J., Gabius, S., Eds.; Chapman & Hall: London, 1997.

(2) (a) Rini, J. M. *Annu. Rev. Biophys. Biomol. Struct.* **1993**, *24*, 551−577. (b) Gabius, H.-J. *Eur. J. Biochem.* **1997**, *243*, 543−576. (c) Hirabayashi, J. *Trends Glycosci. Glycotechnol.* **1997**, *9*, 1−190. (d) Kaltner, H.; Stiersdorfer, B. *Acta Anat.* **1998**, *161*, 162−179. (e) Kopitz, J.; von Reitzenstein, C.; Burchert M.; Cantz M.; Gabius, H. J. *J. Biol. Chem.* **1998**, *273*, 11205-11211. (f) Perillo, N. L.; Marcus, M. E.; Baum, L. G. *J. Mol. Med.* **1998**, *76*, 402−412. (g) Philips, M. L.; Nudelman, E.; Gaeta, F. C. A.; Perez, M.; Singhal, K.; Hakomori, S.; Paulson, J. C. *Science* **1990**, *250*, 1132.

(3) (a) Postema, M. D. H. *C-Glycoside synthesis*; CRC Press: Boca Raton, 1995. (b) *Chemistry of C-glycosides*; Levy, W., Chang, D., Eds.; Elsevier: Cambridge, 1995. (c) Johns, B. A.; Pan, Y. T.; Elbein, A. D.; Johnson, C. R. *J. Am. Chem. Soc.* **1997**, *119*, 4856−4865. (d) Leeuwenburgh, M. A.; Picasso, S.; Overkleeft, H. S.; van der Marel, G. A.; Vogel, P.; van Boom, J. H. *Eur. J. Org. Chem.* **1999**, 1185−1189. (d) Marquis, C.; Picasso, S.; Vogel, P. *Synthesis* **1999**, *SI*, 1441−1452.

(4) Linhardt, R. J.; Vlahov, I. R. *Tetrahedron* **1998**, *54*, 9913−9959.

(5) (a) Weatherman, R. V.; Kiessling, L. L. *J. Org. Chem.* **1996**, *61*, 534. (b) Weatherman, R. V.; Mortell, K. H.; Chervenak, M.; Kiessling, L. L. *Biochemistry* **1996**, *35*, 3619.

(6) Houk, K. N.; Eksterowicz, J. E.; Wu. Y.; Fuglesang, C. D.; Mitchell, D. R. *J. Am. Chem. Soc.* **1993**, *115*, 4170−4177.

(7) (a) Espinosa, J. F.; Cañada, F. J.; Asensio, J. L.; Martín-Pastor, M.; Dietrich, H.; Martín-Lomas, M.; Schmidt, R. R.; Jiménez-Barbero, J. *J. Am. Chem. Soc.* **1996**, *118*, 10862−10871. (b) Rubinstenn, G.; Sinay, P.; Berthault, P. *J. Phys. Chem. A* **1997**, *101*, 2536.

(8) (a) Lemieux, R. U.; Koto, S.; Voisin, D. *Am. Chem. Soc. Symp. Ser.* **1979** *87*, 17−29. (b) Thatcher, G. R. J. *The Anomeric Effect and Associated Stereoelectronic Effects*; American Chemical Society: Washington, DC, 1993. (c) Kirby, A. J. *The anomeric effect and related stereoelectronic effects at oxygen*; Springer-Verlag: Heidelberg, Germany, 1983. (d) Thogersen, H.; Lemieux, R. U.; Bock, K.; Meyer, B. *Can. J. Chem.* **1982**, *60*, 44−65. (e) Tvaroska, I.; Bleha, T. *Adv. Carbohydr. Chem. Biochem.* **1989**, *47*, 45−103. (f) Wiberg, K. B.; Murcko, M. A. *J. Am. Chem. Soc.* **1989**, *111*, 4821−4827. (g) Tvaroska, I.; Carver, J. P. *J. Phys. Chem.* **1995**, *99*, 6234−6241. (h) Cramer, C. J.; Truhlar, D. G.; French, A. D. *Carbohydr. Res.* **1997**, *298*, 1−14.

(9) Martín-Pastor, M.; Espinosa, J. F.; Asensio, J. L.; Jimenez-Barbero, J. *Carbohydr. Res.* **1997**, *298*, 15−47.

(10) (a) Wei, A.; Boy, K. M.; Kishi, Y. *J. Am. Chem. Soc.* **1995**, *117*, 9432−9437. (b) Wang, Y.; Goekjian, P. G.; Ryckman, D. V.; Miller, W. H.; Babirad, S. A.; Kishi, Y. *J. Org. Chem.* **1992**, *57*, 482−489. (c) Wu, T.; Goekjian, P. G.; Kishi, Y. *J. Org. Chem.* **1987**, *52*, 4819−4823. (d) Wei, A.; Kishi, Y. *J. Org. Chem.* **1994**, *59*, 88−96 and references therein.

(11) Ravishankar, R.; Surolia, A.; Vijayan, M.; Lim, S.; Kishi, Y. *J. Am. Chem. Soc.* **1998**, *120*, 11297−11303.

(12) Espinosa, J. F.; Bruix, M.; Jarreton, O.; Skrydstrup, T.; Beau, J.-M.; Jiménez-Barbero, J. *Chem. Eur. J.* **1999**, 442−448.

10.1021/ja9922734 CCC: $18.00
Published on Web 11/24/1999

Chart 1. Schematic Representation of the Three Basic Orientations around ϕ Angle in Glycopyranosides[a]

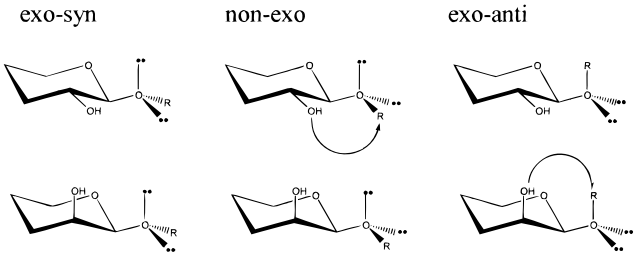

[a] 1,3-Type interactions between OH_2 and R for *manno* and *gluco* configurations at position 2 are indicated.

protein has elicited the claim that the conformational similarity between *O*- and *C*-glycosides is a general phenomenon.[11] On the other hand, we recently reported that similar conformations for *C*- and *O*- glycosides did not persist at least for *C*- and *O*-lactose (β-(1 → 4)-glycosidic linkage)[7a] and for *C*- and *O*-mannobiose (α-(1 → 2)-glycosidic linkage).[12]

This dichotomy has prompted us to study other *C*-glycosyl compounds. *C*-glycosides are key compounds to deduce the relative importance of steric and stereoelectronic effects in the conformational analysis of oligosaccharides. In principle, if the three staggered conformations around the Φ angle of glycopyranosides are considered (Chart 1), it should be expected that the orientation of the hydroxyl group at position C-2 should strongly influence the conformational equilibrium, in the absence of additional stereoelectronic (*exo-anomeric*) effects.[8] For the regular $^4C_1$(D) chairs, there is a 1,3-*syn*-diaxial interaction between one equatorially substituted C-2 (gluco-series) and the aglycon when the *non-exo-anomeric* (*non-exo*) conformation is considered. Such steric interactions do not occur for the *exo-anomeric syn* and *anti* conformations (*exo-syn* and *exo-anti*). In contrast, 1,3-type interactions should be expected for one axially substituted *C*-2 (manno-series) and the aglycon when the *exo-anti* conformation is considered. There are no 1,3-*syn*-diaxial interactions for the *exo-syn* and the *non-exo* conformations. It is obvious that, depending on the value of the stereoelectronic effect, the energy difference among the three rotamers will be different for *O*- and *C*-glycosides. In fact, the separation and the quantitative evaluation of these 1,3-*syn*-diaxial interactions can only be performed in the absence of the *exo-anomeric* effect. Despite X-ray structural evidence as well as a variety of computational studies which prove the existence of the *exo-anomeric* effect,[8] an experimental estimation of the strength of the *exo-anomeric* contribution in water solution is still not available. Ab initio calculations in vacuo have estimated the strength of the *exo-anomeric* effect between 1.5 and 4.0 kcal/mol.[8] On the other hand, Wiberg and co-workers[8f] and Houk and co-workers,[6] using ab initio calculations, have estimated the gauche O−C1−C2−C3 preference to be between 0.3 and 0.8 kcal/mol in simple systems, related to *C*-glycosides.

We suggest that the systematic comparison of β-*C*-linked glycosides having the gluco and manno configurations should provide unambiguous data to verify the importance of steric effects in modulating the conformation around the Φ angle of oligosaccharides. A study of 2-deoxy analogues has led to the conclusion[10b] that: *removal of the 2-hydroxyl group does not fundamentally alter the conformation around the C-glycosidic bond*, ruling out the 1,3-diaxial-like interaction as the primary factor in controlling the conformational behavior of these compounds.[10b] On the other hand, ab initio calculations in vacuo by Houk et al. showed[6] that the relative stabilization of the *exo-syn* vs *non-exo* forms, increased from 0.7 to 2.2 kcal/mol when adding a 3-hydroxyl group to 2-ethyltetrahydropyran to create 1,3-type interactions. According to these data, the 1,3-*syn*-diaxial destabilization should amount to about 1.5 kcal/mol. Our experimental investigation outlined in this paper was designed to reveal the relative importance of the stereoelectronic and steric effects in oligosaccharides and to solve the controversy about similar or dissimilar conformations for *O*-glycosides and their *C*-analogues. Among *C*-glycosides, aza-*C*-disaccharides combine the features of azasugars[13] and *C*-glycosyl compounds.[3c,d,e] They contain the same stereochemical information as the regular hexoses, and in addition, many exhibit potent biological activity. In principle, azasugars are good glycosidase inhibitors due to their ability to mimic the transition-state oxonium ion as a result of the protonation of the intraring nitrogen at physiological pH.[14] In fact, the synthesis of several aza-*C*-disaccharides was recently accomplished, and their inhibition ability was characterized.[3c,d] The observed differences in biological activity were attributed

Chart 2. Schematic Representation of Compounds 1−8

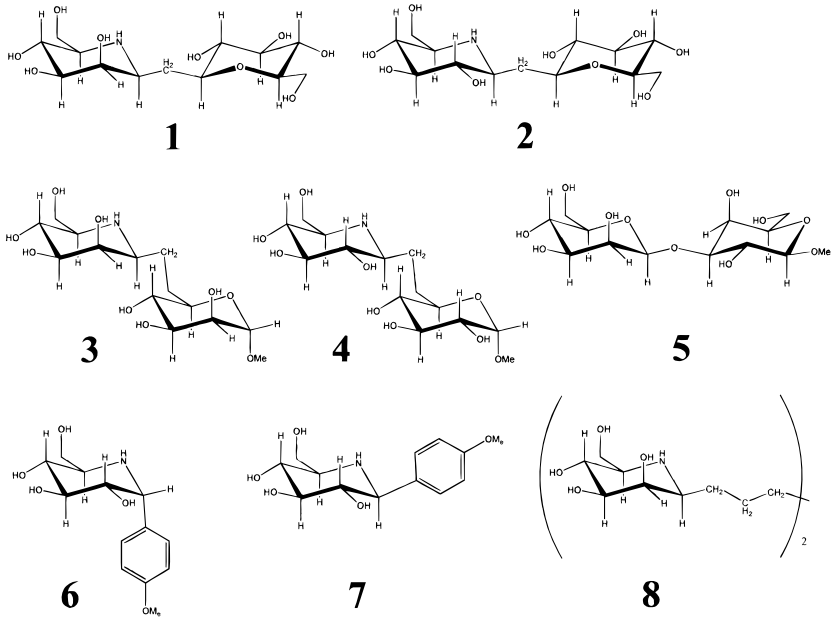

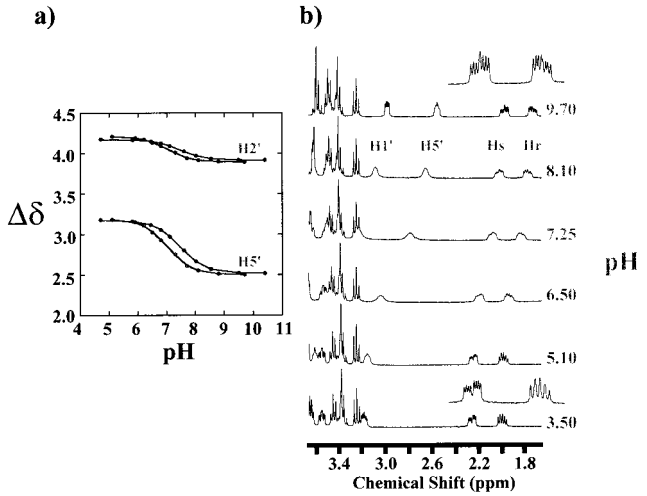

Figure 1. (a) Chemical shift variation of several protons of **1** and **2** upon changing pH and the corresponding pK_a determination. (b) The pH-induced variation of the coupling pattern of **1**.

to the variations in the linkage and stereochemistry of the pyranose portion of the pseudodisaccharides,[3c] On this basis, we report here the conformational study of four different aza-*C*-disaccharide analogues, namely *C*-β-D-azaMan-(1 → 1)-β-D-Glc (**1**), *C*-β-D-azaGlc-(1 → 1)-β-D-Glc (**2**), *C*-β-D-azaMan-(1 → 6)-β-D-Man (**3**), *C*-β-D-azaGlc-(1 → 6)-β-D-Glc (**4**) using NMR spectroscopy and time-averaged restrained molecular dynamics calculations (tar-MD)[15] with the AMBER 5.0 force field.[16] For comparison, conformational energies of a related *O*-glycoside, namely O-β-D-Man-(1 → 3)-D-Gal β-OMe (**5**), were also determined. Moreover, the inhibitory potency of aza-*C*-glycosides **1**−**4** and **6**−**8** (Chart 2) have been tested toward several glycosidases.[3c,d]

Results and Discussion

Titration Studies. As a first step, to deduce the protonation state of the intraring nitrogen of the azasugar units, the pK_a values of compounds **1**−**4** were deduced from ^{1}H NMR titration experiments. An example of the chemical shift changes observed in **1** with varying pH is shown in Figure 1. The measured pK_a's are 7.0, 6.1, 7.5, and 6.2 for **1**, **2**, **3**, and **4**, respectively. Three generalizations can be extracted from the titrations:

(1) The pK_a value of the nitrogen depends on the configuration at *C*-2 of the azasugar moiety. Indeed those disaccharides with azamanno configuration (**1**, **3**) present pK_a values between 0.9 and 1.3 units higher than the azagluco analogues (**2**, **4**).

(2) The proximity of the vicinal glucose moiety influences the pK_a value only for the azamanno disaccharide (**1** vs **3**, 0.5 units) and not for the azagluco analogue (**2** vs **4**).

(3) The vicinal *J* values involving the interglycosidic CH_2 protons showed significant changes upon pH variations, again, only for the (1 → 1)-linked azamanno disaccharide **1** (Figure 1).

With respect to the first observation, the pK_a differences can be explained by the existence of a direct polar interaction between the intraring nitrogen and the O-2 hydroxyl group,

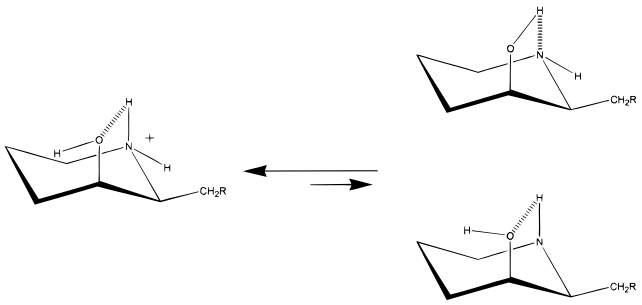

Figure 2. The proposed intraring five-membered ring hydrogen bond interaction for azamanno compound **1**.

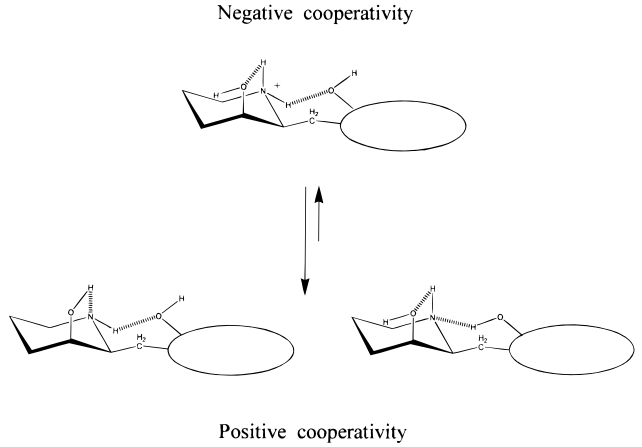

Figure 3. The proposed inter-ring seven-membered ring hydrogen bond/electrostatic interaction for azamanno compound **1**.

which is only possible for manno configurations (Figure 2). The net effect in pK_a is an increase of the basicity of azaMan (**1**, **3**) compared to azaGlc (**2**, **4**) compounds. This fact reflects that the intraresidue five-membered N(+)−H···O interaction in the acid form is favored over the alternatives in the basic form (Figure 2).

With respect to the second experimental observation, the decrease in basicity of the nitrogen of the (1 → 1)-linked **1** in comparison to the (1 → 6)-linked **3**, suggests that additional interactions with the remote sugar residue are taking place especially in **1**. The 0.5 unit decrease in pK_a when passing from **3** to **1** (approaching the vicinal sugar unit) indicates that these additional interactions probably involve an interresidue seven-membered (including the hydrogen) ring O···N hydrogen bond or electrostatic interaction in which the nitrogen acts as proton acceptor (Figure 3). Since the vicinity of the Glc unit in azagluco **2** with respect to azagluco **4** does not influence the pK_a value, the ability of the nitrogen atom to get involved in interresidue interactions is modulated by the configuration at C-2. Although merely speculative, this behavior could be explained by the existence of a cooperative hydrogen bond network as depicted in Figure 3. For manno configurations, the ability of the nitrogen to act as an interresidue proton donor is diminished in the protonated form by the N−H···O interaction, in a case of negative cooperativity.[17] On the other hand, at basic pH values, the ability of the nitrogen to participate as an acceptor (as indicated by the lower pK_a of **1** vs **3**) with the vicinal sugar unit is enhanced by the intraresidue N···O interaction, in a case of positive cooperativity[17] (Figure 3). As a net effect, the closer proximity of the vicinal sugar unit in **1** vs **3** produces a shift in

(13) Elbein, A. *Annu. Rev. Biochem*. **1987**, *56*, 497.
(14) Sinnott, M. L. *Chem. Rev.* **1990**, *90*, 1171.
(15) (a) Torda, A. E.; Scheek, R. M.; van Gunsteren, W. F. *J. Mol. Biol* **1990**, *214*, 223−235. (b) Pearlman, D. A. *J. Biomol. NMR* **1994**, *4*, 1−16. (c) Torda, A. E.; Scheek, R. M.; van Gunsteren, W. F. *Chem. Phys. Lett.* **1989**, *157*, 289−294. (d) Pearlman, D. A. *J. Biomol. NMR.* **1994**, *4*, 279−299.
(16) Pearlman, D. A.; Case, D. A.; Caldwell, J. W.; Ross, W. S.; Cheatham, T. E., III; DeBolt, S.; Ferguson, D.; Siebal, G.; Kollman, P. *Comput. Phys. Commun*. **1995**, *91*, 1−41.
(17) For a survey of hydrogen bonding relevance in sugars, see: Jeffrey, G. A.; Saenger, W. *Hydrogen bonding in biological structures*; Springer-Verlag: Berlin, 1991.

Table 1. Parameters for the Inhibition of Glycosidases by Compounds **1**−**4**, **6**−**8**

enzyme	comd	IC50(mM)	K_i(mM)
amyloglucosidase	**1**	0.08	0.031
amyloglucosidase	**2**	0.05	0.019
amyloglucosidase	**4**	0.009	0.004
amyloglucosidase	**7**	3	1.3
amyloglucosidase	**3**	0.025[a]	
amyloglucosidase	**8**	0.015	0.0045
α-mannosidase	**8**	0.1	*b*
β-glucosidase	**8**	1.75	0.8

[a] From ref 3c. [b] This compound does not behave as a competitive inhibitor. Compound **6** did not show any inhibition against any glycosidase.

the pK_a value. For Glc configurations (**2** and **4**), the lack of pK_a variation indicates that in the absence of cooperativity effects, any seven-membered ring interresidue hydrogen bond is too weak both in the protonated and non-protonated forms. With respect to the third generalization, these facts are also manifested in a slight conformational dependence on pH, especially for azamanno compound **1**. (See below under conformational analysis).

Inhibition Studies. The inhibition abilities of aza-*C*-oligosaccharides **1**−**4**, **6**−**8** (Chart 2) were tested against different glycosidases, using *p*-nitrophenyl glycosides as substrates (Table 1). The compounds were tested up to a maximum concentration of 5 mM. All compounds except **6** inhibited *Aspergillus niger* amyloglucosidase[18] with varying K_i. The bidentate azasugar **8** and the (1 → 6)-linked saccharides[3c,d] **3** and **4** were the best inhibitors by far (IC_{50} 9−25 uM, K_i, 4−4.5 uM). Compound **8** was also the only one to inhibit other glycosidases (see Table 1) although with very weak potency. It appears that the extra distance between the six-membered rings increases the inhibition ability toward *A. Niger* amyloglucosidase (**1** or **2** vs **4**, **8**). In addition, the stereochemistry at position *C*-2 (sugar nomenclature) did not strongly affect the kinetic parameters and both *β*-azaGlc and *β*-azaMan sugars provided similar numbers.[3c] The only α-sugar employed (**6**) did not show any inhibition of the enzymes, suggesting the importance of the stereochemistry at *C*-1 for the activity toward glycosidases.[19] Curiously, the enzyme from *A. niger* is an α-glucosidase. Therefore, some distortion of the six-membered rings could be expected to take place during the inhibition process to properly accommodate the *β*-azaGlc and *β*-azaMan sugars. TR-NOESY experiments[7a] were attempted to gain this information. Unfortunately, no TR-NOESY cross-peaks could be obtained under different experimental conditions and ligand/protein molar ratios. Probably, the off-rate constant was out of the appropriate range to observe exchange-transferred signals. The use of multivalent saccharides to bind lectins has been reported recently and the observed affinities increased several orders of magnitude compared to those of the parent oligosaccharide.[20] Our results seem also to point in this direction when considering the inhibition ability of **8** with other glycosidases.

Conformational Analysis. The ^{1}H NMR chemical shifts are given in Table S1 in the Supporting Information. The chemical shift values in the azaGlc and Glc residues are more similar at acid pH. Because of the basic amino group, analysis of the conformational behavior around the glycosidic bonds of **1**−**4** were performed at pH 3.5 and pH 10.0, which should correspond to positively charged and neutral species, respectively. The intraring vicinal coupling constants[21] proved that all of the six-membered rings adopt the $^4C_1$(D) conformation, independent of the stereochemistry at C-2 and the pH of the medium. Glycosidic torsion angles[22,23] of **1** and **2** are defined as Φ_{aza} $H1_{aza}-C1_{aza}-CH_2-C1_{Glc}$ and Φ_{Glc} $H1_{Glc}-C1_{Glc}-CH_2-C1_{aza}$. Glycosidic torsion angles of **3** and **4** are defined as Φ_{aza} $H1_{aza}-C1_{aza}-CH_2-C6$ and Ψ $C5-C6-CH_2-C1_{aza}$. For Φ_{aza} and Φ_{Glc}, the *exo-syn* conformation is defined as +60°, the non *exo* −60°, and the *exo-anti*, 180°.

Conformation of aza-C-*β*-Man1 → 1*β*-Glc (**1**) and aza-C-*β*-Glc1 → 1*β*-Glc (**2**) in water. As the first step in deducing the conformational behavior[23] of compounds **1** and **2,** their potential energy surfaces were calculated using the MM3* force field; the results are shown in Figure 4. These surfaces just provide a first estimation of the conformational regions which are energetically accessible. The analysis of the maps for **1** (aza-*manno* series) and **2** (aza-*gluco* series) shows the presence of seven conformational families indicating that these compounds are rather flexible (Tables S2−S5 in the Supporting Information, Figure 4). A representation of these families is given in Figure 5. Despite the overall similarity between both maps, the distinct relative energies of the minima for **1** and **2** (Tables S2 and S3 in Supporting Information) indicate that the conformational equilibrium around Φ_{aza} is predicted to be influenced by the orientation of the hydroxyl group at position C-2 of the azasugar ring.

A first conformational description of the Φ_{aza},Φ_{Glc} glycosidic torsions of **1** and **2** was obtained on the basis of the interresidue NOEs[24] and the interglycosidic vicinal proton−proton coupling constants (Tables S2−S5, Supporting Information) that characterize these minima. The key NOEs are $H1_{aza}-H1_{Glc}$, $H1_{aza}-H2_{Glc}$, $H2_{aza}-H1_{Glc}$ and $H2_{aza}-H2_{GLC}$, respectively. The presence of methylene protons at the pseudoglycosidic linkage allowed us to obtain more conformational information with respect to regular *O*-glycosides. Diastereotopic assignment of the prochiral H_R and H_S protons was performed using a protocol similar to that described previously[12] based exclusively on a combination of *J* and NOE values. Once the diastereotopic assignment was performed, up to 12 NOEs (Figures 6 and 7) were unambiguously identified which contain conformational information for both **1** and **2**. The relationship between NOEs and proton−proton distances is also well established[24] and can be worked out at least semiquantitavely, when a full matrix relaxation analysis is considered. Since the corresponding NOE intensities are sensitive to the respective conformer populations, a first indication of the population distribution could be obtained by focusing on these key NOEs.

At either pH, the observed NOEs and *J*'s are not compatible with one unique conformation at any linkage (Tables S2−S5

(18) For a recent review on glycosidases, see: Vasella, A. T.; Heightman, T. D. *Angew. Chem., Int. Ed.* **1999**, *38*, 750.

(19) Winchester, B.; Fleet, G. W. *Glycobiology* **1992**, *2*, 199.

(20) (a) For recent synthesis of glycodendrimers, see: Jayaraman, N.; Nepogodiev, S. A.; Stoddart, J. F. *Chem. Eur. J.* **1997**, *3*, 1193−1199. (b) For increased affinity due to multivalency, see for example: Sigal, G. B.; Mammen, M.; Dahmann, G.; Whitesides, G. M. *J. Am. Chem. Soc.* **1996**, *118*, 3789−3800.

(21) For the relation between H/H couplings and conformation, see: (a) Karplus, M. *J. Chem. Phys.* **1959**, *30*, 11. (b) Haasnoot, C. A. G.; de Leeuw, F. A. A. M.; Altona, C. *Tetrahedron* **1980**, *36*, 2783.

(22) A general survey of conformation of carbohydrates is presented in: French, A. D.; Brady, J. W. *Computer Modelling of Carbohydrate Molecules*; American Chemical Society: Washington, DC, 1990.

(23) For relevant applications of NMR data and calculations in conformation of carbohydrates, see: (a) Harris, R.; Kiddle, G. R.; Field, R. A.; Milton, M. A.; Ernst, B.; Magnani, J. L.; Homans, S. W. *J. Am. Chem. Soc.* **1999**, *121*, 2546−2551. (b) Meyer, B. *Topics Curr. Chem.* **1990**, *154*, 141. (c) Bock, K. *Pure Appl. Chem.* **1983**, *55*, 605. (d) Imberty, A. *Curr. Opin. Struct. Biol.* **1997**, *7*, 617−623. (e) Peters, T.; Pinto, B. M. *Curr. Opin. Struct. Biol.* **1996**, *6*, 710−720.

(24) Neuhaus, D.; Williamson, M. P. *The Nuclear Overhauser Effect in strucutural and conformational analysis*; VCH Publishers: New York, 1989.

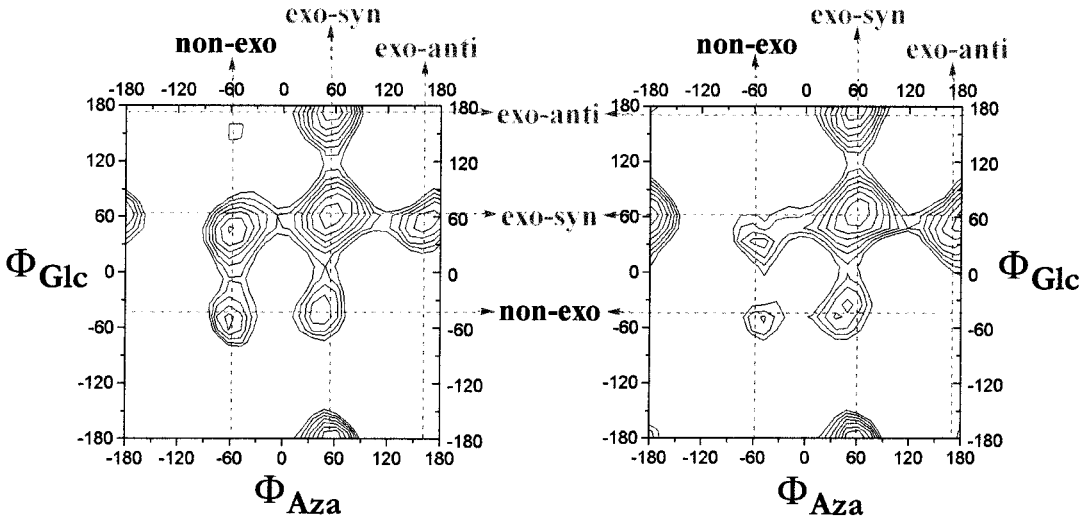

Figure 4. Steric energy maps calculated by the MM3* program with $\epsilon = 80$, (a) for **1** (manno) and (b) for **2** (gluco). Contours are given every 0.5 kcal/mol. The main regions are marked. MM3* predicts different populations of the *non-exo* conformers for both configurations, although it does not fit the experimental data quantitatively.

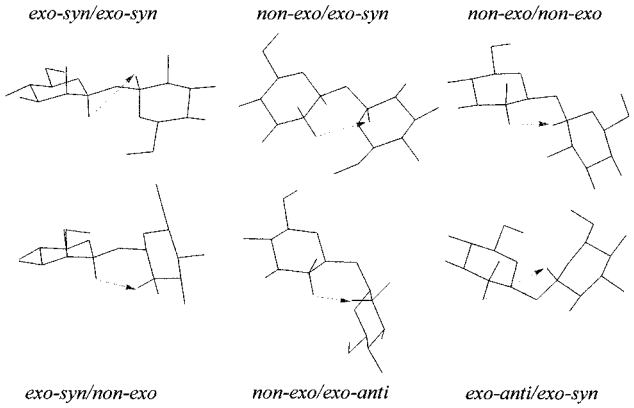

Figure 5. Simplified views of the major low-energy conformations obtained by MM3* calculations for compound **1** Those for compound **2** are similar. Expected key NOEs are indicated for each conformer. Expected *J*'s are indicated in Tables 2 and 3 in the Supporting Information. For Φ_{aza} ($H1_{Aza}-C1_{Aza}-C-C1_{Glc}$) and Φ_{Glc} ($H1_{Glc}-C1_{Glc}-C-C1_{azaman}$), the *exo-syn* conformation is defined as +60°, the *non-exo* −60°, and the *exo-anti*, 180°.

in Supporting Information). In addition, to test the validity of the theoretical MM3* surfaces, the spectroscopic NMR parameters (J and NOEs) of **1** and **2** were calculated from the corresponding probability distributions. No quantitative fit between the experimental and the MM3*-predicted J/NOE values was obtained in any case (Tables S2−S5 in Supporting Information). The availability of up to 12 NOEs and 4 *J*'s with conformational information, permitted the use of time-averaged restrained molecular dynamics (tar-MD)[15,16] to get an *experimentally*-based ensemble average distribution of conformers. Although this method has been employed in nucleic acid and protein NMR structural determination, it has been used rarely in oligosaccharide conformational analysis[22,23] due to the paucity of experimental information usually available. Thus, four tar-MD simulations of **1** and **2** were carried out using the AMBER 5.0 force field,[16] the experimentally derived NOEs and *J*'s, two starting geometries (*exo-syn/exo-syn* and *non-exo/exo-syn*) and two different dielectric constants (1**r* and 80). Following Neuhaus and Williamson,[24] *the ability to fit NOE data using predicted conformations cannot be taken to mean that those conformations are necessarily those that are present; other*

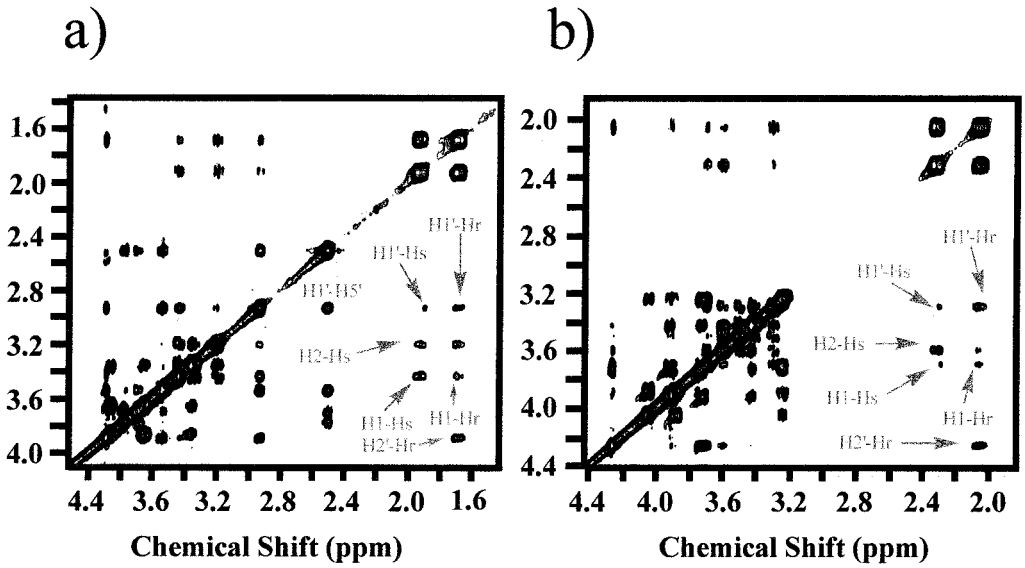

Figure 6. 2D-NOESY spectra of **1** at pH 10.0 (l) and 3.5 (b). (500 MHz, 303 K, D_2O, mixing time, 600 ms. Key NOEs are noted.

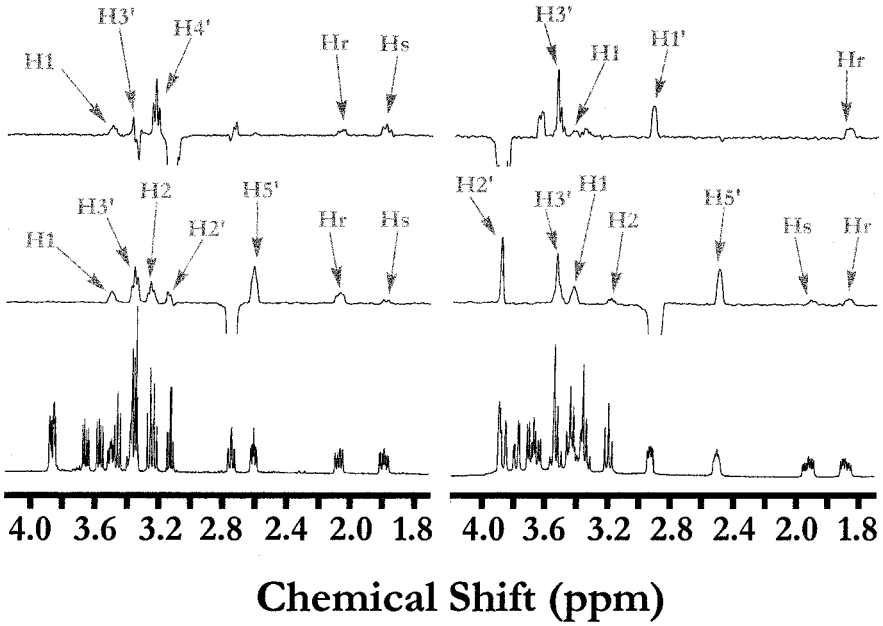

Figure 7. 1D-DPFGSE NOESY spectra of **1** (right) and **2** (left) at pH 10.0. (500 MHz, 303 K, D_2O, mixing time, 800 ms. Key NOEs are noted. Bottom: Regular 1D spectrum. Middle: Inversion of H-1 of the aza-residue. Top: Inversion of H-2 of the aza-residue.

choices might well fit the NOE data also. Nevertheless, the combination of 4 *J*'s and 12 NOEs data to define only two dihedral angles gives confidence in the populations obtained, which, in fact, only modified the MM3* energy surface described above, with different minima populations. The distributions are shown in Figure 8 and the summary of the results gathered in Tables S2−S5 of the Supporting Information.

pH 3.5 (Charged Nitrogen). The trajectories indicate the presence of more than five minima in the distribution (Figure 8) with populations ranking between 5 and 29% for **1** and between 1 and 40% for **2**. Now, all of the NOE-derived distances and *J*-couplings are reproduced in a quantitative manner. A simple visual inspection reveals clear differences for the conformer distribution around Φ_{azaman} and Φ_{Glc} torsions (either aza or not). For Φ_{azaMan}, the minor population is located around the *exo-anti* conformer (7%). The *exo-syn* (50%) and *non-exo* (43%) conformers are almost equally populated. On the other hand, for Φ_{Glc} and Φ_{azaGlc}, the minor population is always located around the *non-exo-anomeric* region (7−9%). The *exo-syn* conformer always dominates the equilibrium (61−73%), and appreciable amounts of the *exo-anti* conformer (18−32%) are also present.

pH 10. (Neutral Nitrogen). According to the trajectories (Figure 8), many minima also contribute to the conformational equilibrium in these conditions. Nevertheless, some differences in the population distributions are observed when increasing pH, especially for compound **1**. These variations are the consequence of the observed changes in both the J couplings and the NOE intensities (Tables S2−S5 in the Supporting Information). For instance, the *J* values which involve azaMan H-1 of **1** ($J_{H1aza-HS}$ 8.8, $J_{H1aza-HR}$ 4.3 Hz), differ in about 2 Hz with those measured at pH 3.5. The populations of the different minima range between 3 and 56% for **1** and between 4 and 46% for **2**.

With these distributions all the experimental data are reproduced in a quantitative manner. Regarding the conformation around Φ angles, with or without nitrogen within the ring, the trend observed at acidic pH is still mantained at pH 10. For Φ_{azaMan}, the minor conformer is *exo-anti* (6%). There is a 20% change in the populations of the *exo-syn* (74%) and *non-exo* (20%) conformers with respect to pH 3.5. For Φ_{azaGlc}/Φ_{Glc} torsions, the major conformer is always the *exo-syn* (68−73%). Now, in contrast with Φ_{azaMan} torsions, the *exo-anti* region is much more populated (17−23%) than the *non-exo-anomeric* one (4−12%).

Summary and Discussion of the Results for 1 and 2. These experimentally based distributions for **1** and **2** show (Figure 8) that the effect of the configuration at *C*-2 of the azasugar and sugar residues on the conformational populations is evident at both pHs. The distributions around Φ_{azaMan} of **1** also depend on the pH of the solution. Nevertheless, in all cases, the minor conformer is that which presents a 1,3-type destabilizing interaction between the hydroxyl group at *C*-2 and the vicinal residue, as described in the Introduction and Chart 1. In particular, when OH-2 is equatorial, the minor conformation is always *non-exo-anomeric* (4−12%). When OH-2 is axial, the *exo-anti* conformer is the less populated one (6−7%). The increase of the *exo-syn* population around Φ_{azaMan} of **1** when increasing pH is consistent with the proposed seven-membered ring (including the hydrogen) electrostatic/hydrogen bond interaction depicted in Figure 3. In fact, the interaction between the intraring nitrogen and O-2 of the vicinal Glc unit is only possible for this conformation. The induced change in population (∼20%, which corresponds to a ΔG of ∼0.4 kcal/mol) can be detected in this compound due to the high flexibility of the glycosidic linkages, with many populated regions of the potential energy map. For other more rigid compounds, a 0.4 kcal/mol change would not be detectable. This energy value is also consistent with the 0.5 units of pK_a change.

Assuming the three ideal staggered orientations (*exo-syn*, *non-exo*, and *exo-anti*) around the pseudoglycosidic torsions and using the experimentally derived populations at both pHs for both compounds, the ΔG values for the rotameric equilibrium may be estimated (Figure 9). The obtained ΔG values show the influence of the configuration at C-2. Indeed, for equatorial OH-2 groups, $\Delta G^{exo\text{-}syn/non\text{-}exo}$ amounts to 1.35 ± 0.35 kcal/mol, while the $\Delta G^{exo\text{-}syn/exo\text{-}anti}$ value is 0.65 ± 0.25 kcal/mol. For axial OH-2 groups, the $\Delta G^{exo\text{-}syn/non\text{-}exo}$ is 0.45 ± 0.35 kcal/mol, while the $\Delta G^{exo\text{-}syn/exo\text{-}anti}$ is now 1.30 ± 0.20 kcal/mol. Figure

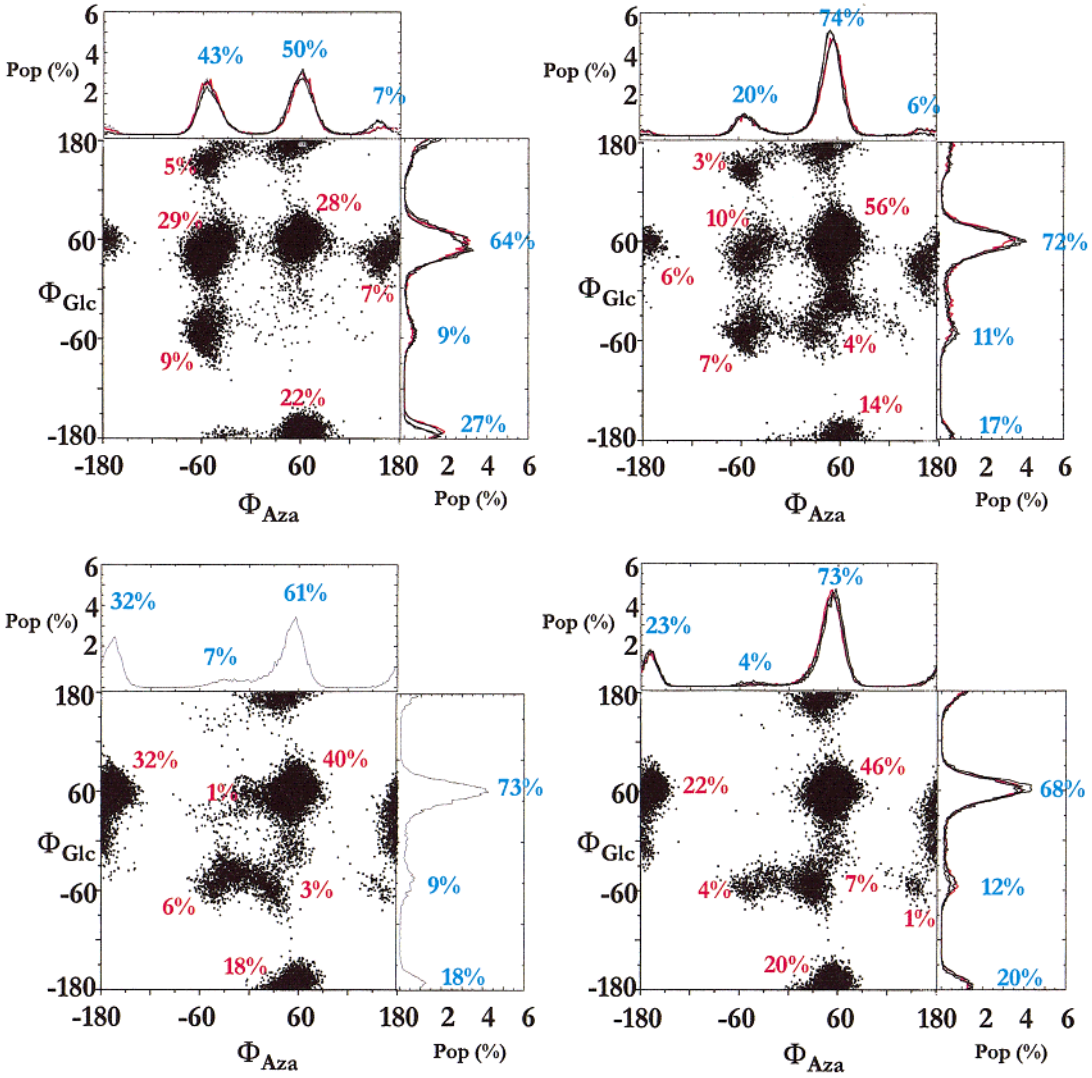

Figure 8. Trajectories of two independent 15 ns tar-MD simulations ($\epsilon = 80$) performed for **1** (top) and **2** (bottom) at acid (left) and basic (right) pH with AMBER 5.0. Four MD simulations were performed in total for each compound. Fourteen NOEs and four coupling constants were included. The agreement between the back-calculated NMR parameters and the observed ones was excellent. The populations of every conformational family are given. The top and right traces show the percentage of populations at any orientation (*exo-syn, non-exo, exo-anti*). The results of two of the simulations are superimposed. The difference between Φ_{aza} of **1** and **2** is evident, especially at low pH.

10 shows schematically the rotameric equilibrium between the three ideal conformers. For *exo-syn* conformers, the OH−2/R interactions can be assumed to be equivalent for both configurations, as depicted in the left-hand side of Figure 10. Therefore, a simple subtraction of the ΔG values allows the direct measurement of the ΔG contribution to the rotation around Φ which arises from the interaction between OH-2 and the vicinal residue R. Thus, the additional $\Delta\Delta G$ cost ($\Delta\Delta G = \Delta G_{Glc}^{exo\text{-}syn/non\text{-}exo} - \Delta G_{Man}^{exo\text{-}syn/non\text{-}exo}$) for the *exo-syn/non-exo* transition of Φ within a sugar with an equatorial hydroxyl group in comparison with an axial one is 1.05 ± 0.15 kcal/mol (Figure 10). In a similar way, the corresponding $\Delta\Delta G$ for the *exo-syn/exo-anti* transition ($\Delta\Delta G = \Delta G_{Glc}^{exo\text{-}syn/exo\text{-}anti} - \Delta G_{Man}^{exo\text{-}syn/exo\text{-}anti}$) is −0.75 ± 0.05 kcal/mol. Both 1,3-*syn*-diaxial interactions as well as other steric and polar effects are contained in these $\Delta\Delta$G values. The existence of a slight influence of polar effects is manifested by the observed influence of pH upon the distribution.

Conformation of aza-*C*-*β*-Man1 → 6Man*β* (3) and aza-*C*-*β*-Glc1 → 6Glc*β* (4). To isolate the effect of the 1,3-*syn*-diaxial interaction, the conformational behavior around Φ_{aza} of the (1 → 6)-linked glycosides **3** and **4** was also studied. Since these compounds have three bonds in the interresidue linkages, no important polar and/or steric interactions, apart from the 1,3-type, between the residues are likely to occur. In fact, it is known that (1 → 6)-linked oligosaccharides are rather flexible around ω and Ψ linkages, due to the few interactions existent between the two residues.[25] Diastereotopic assignment of the prochiral H_R and H_S protons was performed as described previously.[12] The protocol was more complicated as a result of the presence of two contiguous CH_2 units, and we will detail this analysis (Figure 11). The *J*'s for **3** are $J_{H\text{-}1aza,H\text{-}lowfield}$ 8.7 and $J_{H1\text{-}aza,H\text{-}highfield}$ 4.3 Hz at pH 10.0 and $J_{H1\text{-}aza,H\text{-}lowfield}$ 9.3 and $J_{H1\text{-}aza,H\text{-}highfield}$ 4.2 Hz at pH 3.5, indicating the existence of a predominant conformation with an *anti*-type relationship between $H\text{-}1_{azaman}$ and $H_{lowfield}$, and a *syn*-type arrangement between $H\text{-}1_{azaman}$ and $H_{highfield}$, at both pHs. If we consider the two possible staggered rotamers around Φ_{aza} with this arrangement (Figure 12), it is obvious that for the *exo-anomeric syn* conformation there is close proximity between the proton *syn* to $H\text{-}1_{azaman}$ and $H\text{-}2_{azaman}$. In contrast, for the *non-exo-anomeric* orientation, there is close proximity between C-6 and $H\text{-}2_{azaman}$.

(25) Dowd, M. K., Reilly, O. J.; French, A. D. *Biopolymers* **1994**, *34*, 625−638.

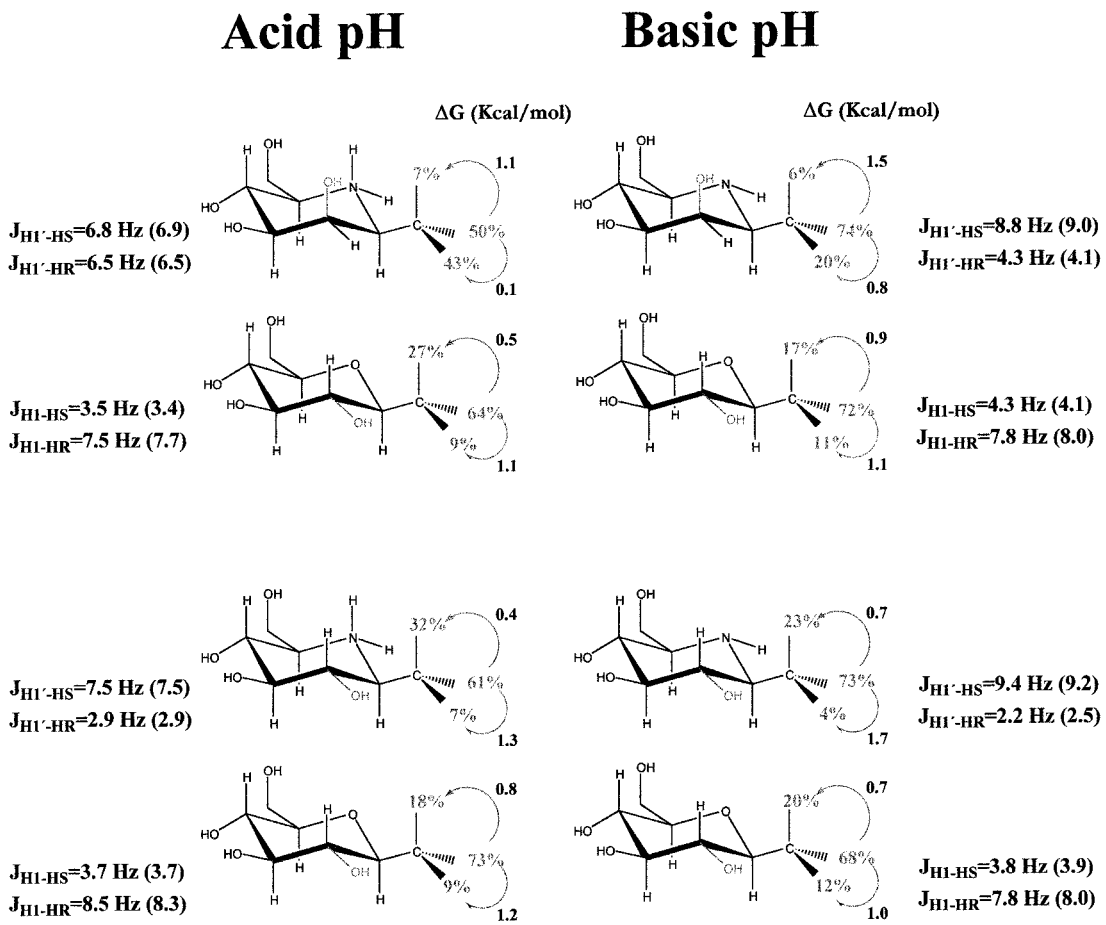

Figure 9. Representation and relative free energies of the rotameric equilibrium at acidic and basic pHs for the different torsion angles of **1** and **2**. The experimental *J* values for the methylene protons and the tar-MD predicted couplings are shown in parentheses.

Medium-strong NOEs were observed between H-2_{azaman} and both H-$6_{R,S}$ of the remote sugar moiety (Figure 11). Indeed, these NOEs are even stronger than those between H-1_{azaman} and H-$6_{R,S}$, indicating that the *non-exo-anomeric* orientation around Φ_{aza} of **3** is highly populated in solution.[3e] The assignment of $H_{lowfield}$ (8.7, 9.3 Hz) is therefore H_S and $H_{highfield}$ is H_R (4.3, 4.2 Hz). Note the difference in Cahn−Ingold−Prelog order of the substituents in **3** with respect to **1**. Once the diastereotopic assignment was performed, the *J* values and the NOE-derived distances were included in the tar-MD protocol as described above (Figure 13, Table S6 in Supporting Information). The population of the *non-exo* conformer is about 75% at either pH. Regarding the conformation around the C5−C6 linkage, two strong H-5 to both H-6_{RS} NOEs were observed, which together with two small $J_{H5,H6RS}$ couplings indicates the presence of a major *gg* rotamer around the C5−C6 hydroxymethyl chain. The same protocol was used for compound **4** (azaGlc configuration). In this case, the data could only be obtained at pH 10.0, ($J_{H1\text{-}aza,HR}$ 8.0 Hz and $J_{H1\text{-}aza,HS}$ 3.2 Hz) providing evidence of a major *exo-anomeric syn* orientation (62−70%). A Glc-typical conformational equilibrium[22,23] *gg:gt* for the C5−C6 hydroxymethyl group was also deduced from NOE/*J* analysis. Therefore, the results obtained for **3** and **4** for both Φ_{aza} angles are similar to those reported above for **1** and **2**, respectively. Nevertheless, the data for **3** indicate a higher percentage of *non-exo* conformers in comparison with **1**. Indeed, the absence of interactions between the azaMan residue and the remote sugar unit of **3** increases the amount of *non-exo* conformers (now 72% at either pH). Following the protocol described above to estimate $\Delta\Delta G$ values, it can be deduced that the isolated 1,3-type interaction produced an energy cost of 1.7 ± 0.1 kcal/mol ($\Delta\Delta G = \Delta G_{Glc}^{exo\text{-}syn/non\text{-}exo} - \Delta G_{Man}^{exo\text{-}syn/non\text{-}exo}$) for the *exo-syn/non-exo* transition and of −0.7 ± 0.4 kcal/mol ($\Delta\Delta G = \Delta G_{Glc}^{exo\text{-}syn/exo\text{-}anti} - \Delta G_{Man}^{exo\text{-}syn/exo\text{-}anti}$) for the *exo-syn/exo-anti* transition. This 1.7 ± 0.10 kcal/mol energy value for the 1,3-*syn*-diaxial interaction between an equatorial OH and the aglycon is in excellent agreement with the ab initio results reported by Houk et al. for an equivalent interaction in 2-ethyl-3-hydroxytetrahydropyran (1.5 kcal/mol) in vacuo.[6]

There has been some controversy about the conformational similarity between *O*- and *C*-glycosides.[7,10−12,26,27] The results described above have demonstrated that the conformation of *C*-glycosides is primarily governed by 1,3-type interactions and, additionally, unambiguously confirm the existence of major flexibility around their glycosidic linkages. This flexibility is evidenced not only around the aglyconic Ψ angle[7] but also around Φ. In particular, the flexibility is more clearly experimentally characterized when sugars of the *β-C*-manno series are compared with their *β-C*-gluco analogues. Slight dependence of the conformational equilibrium on pH (due to polar effects) is observed, at least for aza-*C*-glycosides.

Regarding the question of whether *C*-glycosides reproduce the conformational behavior of natural *O*-glycosides, our results indicate that, in principle, there is not a general answer. As mentioned above, *C*-glycosides are always more flexible than their parent *O*-analogues, and this has been already demonstrated for the different behavior around Ψ angle. Regarding the degree of similarity around Φ, for *β-C*-gluco or *β-C*-galacto (with equatorial OH-2) analogues, the conformational distribution around this angle resembles, although only in a qualitative manner, the distribution for *β-O*-glycosides with a major *exo-anomeric syn* orientation.[8] However, for the *β-C*-analogues

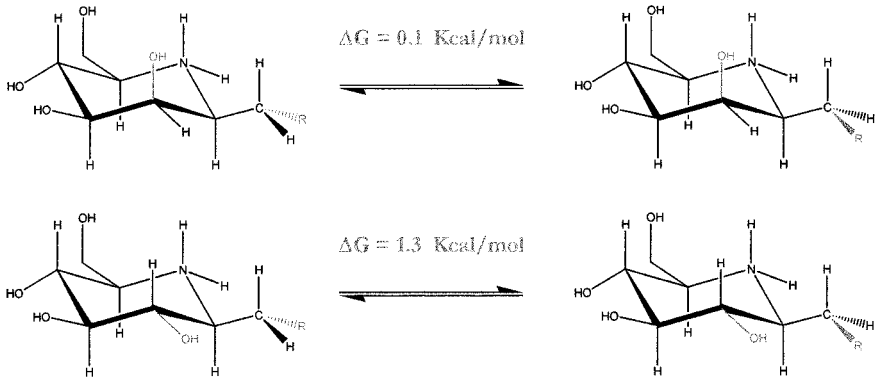

Acid pH (*exo-syn/non-exo*): $\Delta\Delta G = \Delta G_{glc} - \Delta G_{man} = 1.3\text{-}0.1 = 1.2$ Kcal/mol

Basic pH (*exo-syn/non-exo*): $\Delta\Delta G = \Delta G_{glc} - \Delta G_{man} = 1.7\text{-}0.8 = 0.9$ Kcal/mol

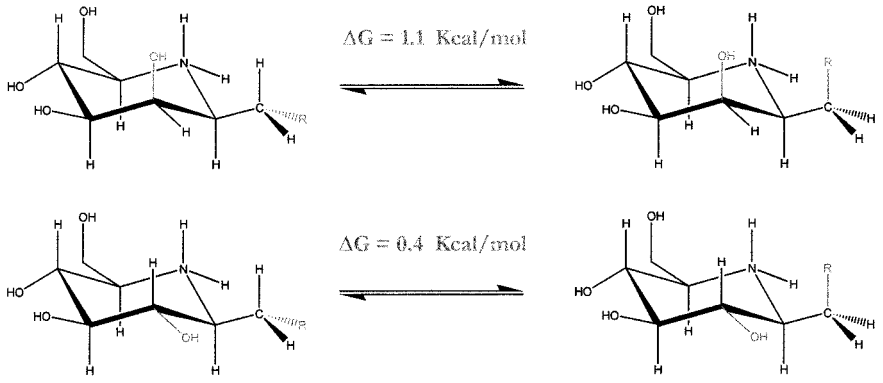

Acid pH (*exo-syn/exo-anti*): $\Delta\Delta G = \Delta G_{glc} - \Delta G_{man} = 0.4\text{-}1.1 = -0.7$ Kcal/mol

Basic pH (*exo-syn/exo-anti*): $\Delta\Delta G = \Delta G_{glc} - \Delta G_{man} = 0.7\text{-}1.5 = -0.8$ Kcal/mol

Figure 10. Representation of the additional $\Delta\Delta G$ cost for the *exo-syn/non-exo* and *exo-syn/exo-anti* transitions of Φ within a sugar with an equatorial hydroxyl group at *C*-2 in comparison with an axial one.

important contributions of *exo-anti* (between 17 and 32%) and detectable participation of *non-exo* (between 4 and 12%) conformers are also manifested, in contrast with the almost exclusive participation of *exo-syn* conformers in *O*-glycosides. On the other hand, the β-manno-*C*-glycosides (with axial OH-2), largely deviate from the behavior usually observed in *O*-glycosides[8] by having up to 43% of the *non-exo* rotamer.

Although the energy values of 1,3-*syn*-diaxial interactions described above have been obtained for aza-*C*-glycosides, the corresponding values will be similar for regular *C*-analogues and somewhat larger for the corresponding *O*-glycosides because the *C*−O bonds are shorter than the *C*−*C* bonds. For *O*-glycosides, it is obvious that the *exo-anomeric* effect will be superimposed onto these factors.

The conformational behavior of a β-linked mannopyranoside **5** was also studied to access the energetic contribution of the stereoelectronic effect. A β-mannoside was chosen since according to the data presented above, there are basically no 1,3-type interactions for either the *exo*-syn or *non-exo* forms. Thus, the conformational equilibrium around Φ should be primarily governed by the *exo-anomeric* contribution.

Conformation of O-β-Man1 → 3Galβ-OMe (5) in Water Solution. Compound **5** was also chosen since it presents two proton−proton distances sensitive to *non-exo-anomeric* populations, which in turn could be detected by NOE experiments.[24] In particular, the H-2 Man/H-3 Gal distance is exclusive (2.2 Å) for the *non exo-anomeric* conformer. This distance is 4.2 Å for the *exo-anomeric syn* region. In addition, H-1 Man/H-4 Gal is 3.7 Å for the *exo-syn* and 2.5 Å for the *non-exo* conformer. There is one additional (H-1 Man/H-3 Gal) distance, but this cannot be used to distinguish between conformers since is short in both of them. The potential energy surface calculated for **5** using the MM3* force field is shown in Figure 14. Glycosidic torsion angles are now defined as $\Phi_H = H1_{Man}-C1_{Man}-O-C3_{Gal}$ and $\Psi_H = H3_{Gal}-C3_{Gal}-O-C1_{Man}$. The analysis of the map of **5** (*manno* series) shows that now only one minimum dominates the surface (Figure 14): The global *exo-anomeric* minimum A has dihedral angles of $\Phi_H = 52 \pm 20°$ and $\Psi_H = 5 \pm 30°$ and about 99% of population is located around this conformer. Additional minima B ($\Phi_H = -52 \pm 20°$ and $\Psi_H = 0 \pm 30°$) and C ($\Phi_H = 52 \pm 20°$ and $\Psi_H = 180 \pm 10°$) are almost nonexistent. The negligible contribution of minimum C to the conformational equilibrium of **5** (although this geometry is also favored by the *exo-anomeric* effect) according to MM3* calculations can be easily explained by the existence of two destabilizing steric gauche-type interactions between the aglycon and O5/C2 atoms as well as one 1,3-*syn*-diaxial interaction with the OH at position 2 of the azasugar ring. The conformational description of the glycosidic torsions of **5** can be performed on the basis of the above-mentioned NOEs (Table S7 in the Supporting Information, Figure 15). A full matrix relaxation analysis of the NOEs, together with the absence of NOE between $H2_{Man}-H3_{Gal}$ (Figure 15) indicates that the existence of *non-exo* conformers around Φ_{Man} is below experimental detection. In this case, the MM3* surface quantitatively reproduces the NOE data, and therefore, the major contribution

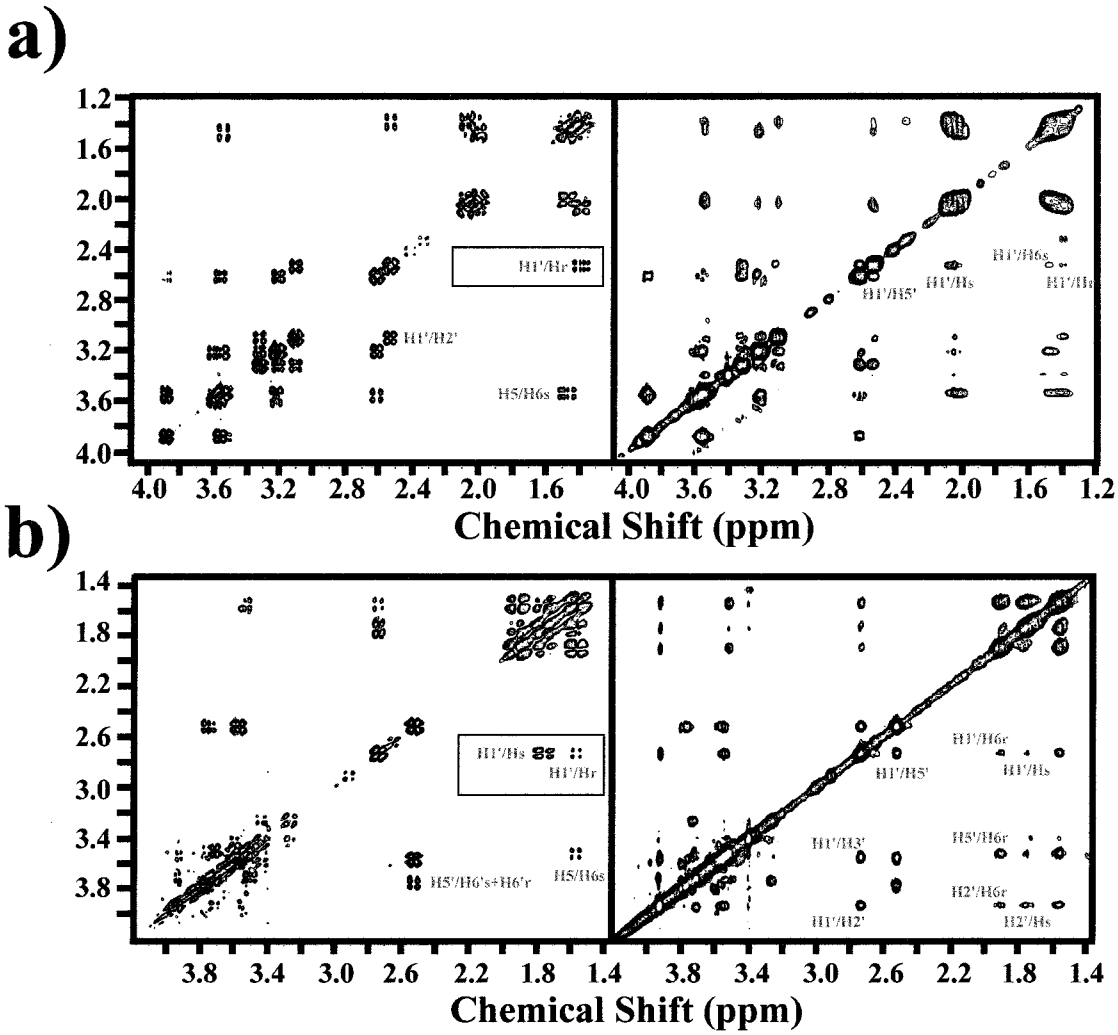

Figure 11. 2D-COSY and NOESY (mixing time 700 ms) spectra of **4** (a) and **3** (b) at pH 10.0 (500 MHz, 303 K, D_2O). Key *J*-cross-peaks and NOEs are noted.

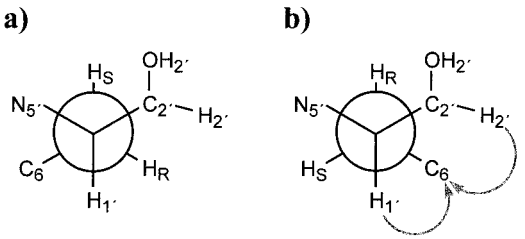

Figure 12. Possible arrangements around Φ_{aza} which can be used to obtain the diastereotopic assignment of the prochiral CH_2 protons of compound **3**.

of the *exo-syn* conformation, with >99% population, is confirmed. According to both NMR and molecular mechanics calculations, there is at least a ~99:1 ratio in favor of the *exo-syn* conformer versus the *non-exo* analogue, which represents a $\Delta G^{exo\text{-}syn/non\text{-}exo}$ of at least 2.75 kcal/mol.

The azaman $\beta(1 \rightarrow 1)$ analogue (**1**) shows an approximate $\Delta G^{exo\text{-}syn/non\text{-}exo}$ of only 0.45 kcal/mol, favoring the *exo*-conformer. Moreover, the azaman $\beta(1 \rightarrow 6)$ analogue (**3**) shows a $\Delta G^{exo\text{-}syn/non\text{-}exo}$ of −0.3 kcal/mol, even favoring the *non-exo-anomeric* conformer. Therefore, assuming similar steric interactions for both *exo-syn* and *non-exo* conformers (indeed, very minor for these compounds) around Φ_{Man} of **1**, **3**, and **5**, the additional stabilization of the *exo-anomeric syn* conformation provided by the stereoelectronic effect in *O*-glycoside **5** in water amounts to at least 2.3 kcal/mol.

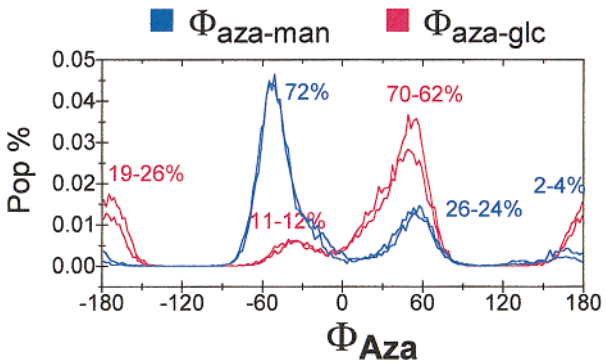

Figure 13. Trajectories of Φ_{aza} for two independent 15 ns tar-MD simulations ($\epsilon = 80$) performed for **3** (blue) and **4** (red) at basic pH with AMBER 5.0. Four MD simulations were performed in total for each compound. Six NOEs and four coupling constants were included. The agreement between the back-calculated NMR parameters and the observed ones was excellent. The populations of every conformational family are given. The difference between Φ_{aza} of **3** and **4** is evident.

Conclusions

The experimental NMR results demonstrate a different conformational behavior of aza-*C*-mannosides **1** and **3** with respect to aza-*C*-glucosides **2** and **4** which strongly depends on the configuration at *C*-2 of the azasugar residue. 1,3-*syn*-diaxial interactions of equatorially oriented hydroxyl groups with the aglycon destabilize (at least 1.0 kcal/mol) the *non-exo-anomeric*

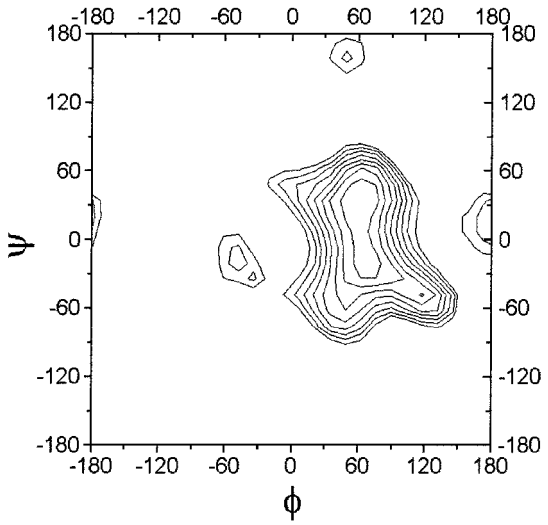

Figure 14. Steric energy maps calculated by the MM3* program with $\epsilon = 1$ and GBSA (H_2O) model for treatment of solvation, for **5** (manno). Contours are given every 0.5 kcal/mol.

conformers around Φ. In contrast, when the conformational distribution around Φ_{aza} of *C*-mannoside **1** is compared with that of *O*-mannoside **5**, it is observed that the *exo-anomeric syn* conformation is additionally stabilized by at least 2.3 kcal/mol. Moreover, the difference between *O*- and aza-*C*-glycosides is due to the C-linkage, not to the azasugar. Thus, if the orientation around Φ_{Glc} (with intraring oxygen) of **1** and **2** is considered, a higher limit of 1.2 kcal/mol is obtained for the energy difference between the *exo-syn* and *non-exo* conformers, *even* with the existence of a 1,3-type interaction for the *non-exo* conformer around this linkage. This value is also very much below (at least 1.1 kcal/mol) the observed difference for **5**.

The demonstration of the existence of an important stereoelectronic stabilization for the *exo-syn* conformer of *O*-glycoside **5** has been achieved. The importance of the *exo-anomeric* effect[8] as the major factor why *O*-glycosides adopt their particular conformation has been questioned.[10,11] Our results indicate that in the absence of stereoelectronic stabilization high populations of conformers which are not consistent with the *exo-anomeric* disposition may be adopted. This fact indicates that the *exo-anomeric* effect is indeed a key factor to determine the conformational behavior of Φ angles of *O*-glycosides in water solution (>2.3 kcal/mol). Moreover, the addition of the *exo-anomeric* and 1,3-effects in *O*-glycosides with an equatorial *O*-2 of the common natural series β-gluco and β-galacto provides the explanation for the unique existence of *exo-anomeric* conformations around Φ in these natural glycosides (>3.3 kcal/mol).

Regarding the use of *C*-glycosides as *O*-glycoside isoesters, it is evident that, due to the low-energy difference among conformers, conformations different from the major one existing in solution may be bound by the binding site of proteins without major energy conflicts. These results, along with those previously obtained for *C*-lactose (with a β-glycosidic linkage), are important for drug design.[7,26,27] Evidently, topological features of the protein binding site restricting ligand mobility and demanding conformer selection, as well as the shifting of the inherent dynamic equilibrium of the flexible *C*-glycoside, can contribute to the final results. When a lectin imposes a constraint by establishing interactions to both sugar units, then the mobility will decrease and only a certain, topologically favored conformer will fit into the binding site. Alternatively, the possibilities still exist that the intramolecular mobility could be maintained, if the entropic penalty exceeds the enthalpic gain by weak sugar−protein interactions, or that the conformation of the global minimum reaches an optimal ΔG value, as seen in the case of ricin.[7a,26] Consequently, the flexibility of *C*-disaccharides may be a limitation to their use as therapeutic agents. Nevertheless, these compounds are still excellent probes to study the combining sites of proteins and enzymes,[27] as well as test compounds to access conformational properties of saccharides.

Experimental Section

Compounds. The synthesis of compounds **1**, **3**[3c], and **8**[28] have been described previously.[3c] Details of the synthesis of **2**, **4**, **6**, and **7** will be published elsewhere.[29] Recently an independent synthesis of compound **4** has been reported.[3d]

Enzymatic Assays. The enzymatic activities of amyloglucosidase (*A. niger*), α-mannosidase (Jack bean), and β-glucosidase (almonds) were determined by monitoring the release of *p*-nitrophenol (PNP) when *p*-nitrophenyl-α-D-glucoside, *p*-nitrophenyl-α-D-mannoside, and *p*-nitrophenyl β-D-glucoside, respectively, were used as substrates.[30] Enzymes and substrates were purchased from Sigma Chemical Co. The reactions for each substrate were carried out in 50 μL of 50 mM sodium acetate buffer (pH 5.6), using different inhibitor concentrations (0.01−5 mM), and started with the addition of the corresponding enzyme at 310 K. After 20 min the reactions were stopped by adding 300 μL of 1 M sodium carbonate, and the amount of released PNP was measured at 400 nm by using a Perkin-Elmer spectrophotometer. Kinetic parameters were calculated by fitting the initial velocities at six concentrations of every inhibitor, by using the Sigmaplot program. A competitive inhibition mechanism was assumed.

Molecular Mechanics and Dynamics Calculations. Molecular mechanics calculations were performed with MM3*[31] as included in MACROMODEL 4.5[32] as described.[7a,12] A dielectric constant $\epsilon = 80$ was used.

For the MD simulations, compounds **1**−**4** were built using the X-Leap[33] program. Atomic charges were derived from AM1 semiempirical calculations. All molecular dynamics simulations were carried out using the Sander module within the AMBER 5.0 package. As a first step, several unrestrained MD simulations were run for all the disaccharides, starting from different low-energy geometries and using different values for the dielectric constant ($\epsilon = 1*r$ and $\epsilon = 80$). No quantitative fit of the experimental data was achieved in any case.

Therefore, MD-tar simulations were carried out for compounds **1**−**4**. NOE-derived distances were included as time-averaged distance constraints and scalar coupling constants as time-averaged *J* coupling restraints. A $\langle r^{-6}\rangle^{-1/6}$ average was used for the distances and a linear average was used for the coupling constants. The *J* values are related to the torsion τ by the well-known Karplus relationship[21a]

$$J = A\cos^2(\tau) + B\cos(\tau) + C$$

A, *B*, and *C* values were chosen to fit the extended Karplus−Altona relationship[21b] for every particular torsion. At the end of the simulations

(26) Espinosa, J. F.; Cañada, F. J.; Asensio, J. L.; Dietrich, H.; Martín-Lomas, M.; Schmidt, R. R.; Jiménez-Barbero, J. *Angew. Chem., Int. Ed. Engl.* **1996**, *35*, 303−306.

(27) Espinosa, J. F.; Montero, E.; Vian, A.; Garcia, J. L.; Dietrich, H.; Martín-Lomas, M.; Schmidt, R. R.; Imberty, A.; Cañada, F. J.; Jiménez-Barbero, J. *J. Am. Chem. Soc.* **1998**, *120*, 10862−10871.

(28) Johns, B. A.; Johnson, C. R. *Tetrahedron Lett.* **1998**, *39*, 749−752.

(29) Johnson, C. R.; Kozak, J.; Zhu, Z., to be published.

(30) Tropea, J. E.; Molyneux, R. J.; Kaushel, G. P.; Pan, Y. T.; Mitchell, M.; Elbein, A. D. *Biochemistry* **1989**, *28*, 2027.

(31) Allinger, N. L.; Yuh, Y. H.; Lii, J. H. *J. Am. Chem. Soc.* **1989**, *111*, 8551−8558. The MM3* force field implemented in MACROMODEL differs of the regular MM3 force field in the treatment of the electrostatic term since it uses charge−charge instead of dipole−dipole interactions.

(32) Mohamadi, F.; Richards, N. G. J.; Guida, W. C.; Liskamp, R.; Caufield, C.; Chang, G.; Hendrickson, T.; Still, W. C. *J. Comput. Chem.* **1990**, *11*, 440−467.

(33) Schafmeister, C. E. A. F.; Ross, W. S.; Romanovski, V. *LEaP*; University of California: San Francisco, 1995.

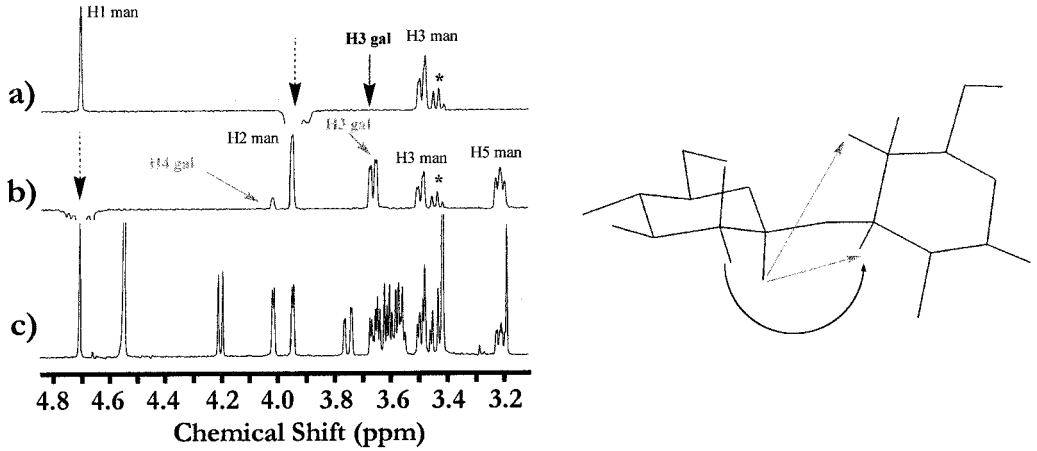

Figure 15. Left: 1D-DPFGSE NOESY spectra of **5** at 500 MHz, 303 K, D_2O, mixing time, 800 ms. Key NOEs are noted. (a) Inversion of H-2 of the Man residue. (b) Inversion of H-1 of the Man residue. (c) Regular 1D spectrum. Right: Schematic representation of the main conformation of **5**. Observed NOEs are indicated in gray. Non-observed NOEs are indicated in black.

the averaged *J* values were calculated using both the regular Karplus and the complete Altona equations and compared to the experimental ones.

Trial simulations were run using different simulation lengths (between 1 and 15 ns) and different force constants for the distances (between 10 and 30 kcal/mol Å^2) and *J* couplings (between 0.1 and 0.3 kcal/mol Hz^2) constraints. Different values for the exponential decay constant (between 100 ps and 1.5 ns) were also tested. These preliminary runs showed that for flexible molecules as **1**−**4,** the use of exponential decay constants shorter than 1 ns produced unstable trajectories and led in some cases to severe distortions of the pyranose rings. In contrast, good results were obtained when using exponential decay constant values of 1 ns or larger. It has been estimated[15c] that simulation lengths of ∼1 order of magnitude larger than the exponential decay constant should be used to generate reliable estimates of average properties. Thus, the final trajectories were run using an exponential decay constant of 1.5 ns and a simulation length of 15 ns.

It is also known[15d] that, when using large force constants for the *J* coupling constraints, the molecule can get trapped in high energy, physically improbable, incorrect minima. To solve this *false minima* problem, low values (between 0.1 and 0.3 kcal/mol Hz^2) were used for the *J* coupling restraints force constants.

Two final 15 ns MD-tar simulations (starting from different low-energy conformations) were run for each disaccharide in both the protonated and nonprotonated forms. Population distributions obtained starting from different initial geometries were almost identical, indicating that the simulation length is adequate for a proper convergence of the conformational parameters. Average distance and *J* values obtained in this way were found to correctly reproduce the experimental ones.

NMR Spectroscopy. The NMR experiments were recorded on a Varian Unity 500 spectrometer. 2-D NOESY experiments used the standard sequence, while 1-D selective NOE spectra were acquired using the double echo sequence proposed by Shaka and co-workers.[34] Five different mixing times were used for the 1-D NOE experiments: 200, 400, 600, 800, and 1000 ms. NOESY back calculations were performed as described.[7a,12]

Acknowledgment. Financial support by DGICYT (Grant PB96-0833) and TMR-EU (FMRX-CT98-0231) is gratefully acknowledged. The work at Wayne State University was supported by a grant (CHE-9801679) from the National Science Foundation. J.L.A. thanks CAM and MEC for fellowships. A.G. thanks GV for a fellowship. We thank Dr. C. Vicent and Dr. P. M. Nieto for discussions. We also thank Dr. P. Vogel (U. of Lausanne) for discussing results prior to publication. This paper is dedicated to Professor P. Sinäy on the occasion of his 62nd birthday.

Supporting Information Available: Tables S1−S7 with the H NMR assignments of compounds **1**−**4** and the details of the molecular mechanics and MD-tar calculations (PDF). This material is available free of charge via the Internet at http://pubs.acs.org.

JA9922734

(34) Stott, K.; Stonehouse, J.; Keeler, J.; Hwang, T.-L.; Shaka, A. J. *J. Am. Chem. Soc.* **1995**, *117*, 4199.